



Evaluation of thermal performance in pulsating heat pipe cooling system

Kushal Guragain^{a,*}, Prakash Badu^a, Sunita Chettri^a, Kapil Baral^a, Durga Bastakoti^a and Rajesh Bhattarai^a

^aDepartment of Mechanical and Automobile Engineering, Pashchimanchal Campus, IOE, TU, Nepal

ARTICLE INFO

Article history:

Received 26 Oct 2023
Revised in 15 Nov 2023
Accepted 14 Dec 2023

Keywords:

Computational Fluid Dynamics
Numerical modeling
Thermal resistance
Pulsating heat pipe

Abstract

The effectiveness of the pulsating heat pipe's is one of many concerning factor in accessing thermal performance is contingent on various physical parameters, namely diameter, length, numbers of turn, heat inputs, and fill ratios of the heat pipe. Both experimental and numerical modeling approaches were employed to investigate a single-loop heat pipe, aiming to determine the thermal resistance at fill ratios of 40%, 50%, and 60% for water. This investigation was conducted under conditions of fluctuating temperature inputs, specifically at 378K, 383K, 388K, and 393K. The experiment was conducted for a copper pipe of inner diameter 4.0625mm and, at the evaporator heat input was supplied 45W. It was found experimentally that the thermal resistance was lowest for the case of 60% FR at 393K (i.e., 0.762K/W) after all the systems were stable but initially at the startup phase thermal resistance was lowest for the case of 50% at 393K (i.e., 1.279K/W). The analysis through numerical simulation included the examination of the temperature variation between the evaporator (T_e) and condenser (T_c), thermal resistance (R_{th}), the pulsating nature of the heat pipe, phase change of the working fluid, and fluid flow behavior. The thermal resistance obtained through numerical modeling is found to be lowest for a 50% FR at 393K (i.e., 1.032K/W) which resembles the initial startup phase. To confirm the occurrence of a two-phase phenomenon inside the PHP, the volume fraction of water in evaporator region was obtained from simulation results and was plotted against the time step. Observation of the oscillating motion in the PHP was conducted through a numerical model and affirmed by the upward movement of the vapor bubble toward the condenser, as well as the velocity vector contour at a specific cross-section of the pipe. The fluctuation in temperature observed in both the evaporator and condenser provides evidence that the liquid and vapor slugs oscillate along the pipe, facilitating the transport of heat from evaporator section to condenser. This experiment suggests that the best case within the tested working condition is for a 60% FR at 393K.

©JIEE Thapathali Campus, IOE, TU. All rights reserved

1. Introduction

Operating passively, the Pulsating Heat Pipe (PHP) efficiently exchanges heat from one point to another, utilizing the phenomenon of change of phases of the working fluid, which is filled in a predefined volumetric ratio. Devised and patented by H. Akachi in the 1990s, the pulsating heat pipe, also recognized as an Oscillating Heat Pipe (OHP), comprises three primary regions: the evaporator, adiabatic region, and condenser. The motion of the slug and plug of the working fluid within

the pipe, induced by evaporation, serves as the driving force in this system[1]. Since its inception, the pulsating heat pipe has garnered attention for its promising applications in diverse fields, including solar-thermal energy management, battery thermal deployment systems, aerospace thermal management systems, waste heat recovery, and electron cooling[2].

The pulsating heat pipe operates with a distinctive mechanism that contributes to its functional advantages. Once stable parameters are attained, the pulsating motions of plugs of liquid and slugs of vapor propel the working fluid through the pipe[3]. Surface tension and the capillary diameter of the pipe lead to the formation and random distribution of plugs and slugs along

*Corresponding author:

 (123guragain123@gmail.com) (K. Guragain)

the pipe. In the realm of pulsating heat pipes, two distinct variations prevail: open loop PHP, characterized by unconnected tube ends, where a singular elongated tube is intricately bent into multiple turns, sealing both ends after the supplied working fluid is introduced and the closed loop PHP, featuring interconnected tube ends forming an endless loop, ensuring a ceaseless movement in circulation direction of the working fluid throughout the PHP's entire operation[4]. Hence, despite the straightforward design of pulsating heat pipes, the interplay between thermo-hydro-dynamic effects throughout the heat and mass transfer process complicates the operational mechanism, rendering it intricate and challenging to fully unveil [5].

Research work involving experimental and theoretical approach has been conducted on heat pipes studying their complex characteristics over decades. In the experimental modeling domain, an in-depth examination of geometric parameters such as critical diameter, cross-sectional area, evaporator and condenser length, adiabatic region, and the number of turns has been undertaken. Simultaneously, a comprehensive exploration of operational parameters, including heat flux, fill ratio, charge flux, inclination angle, and the choice of working fluid, has been conducted[3]. Numerous models capturing the dynamics within closed-loop PHPs have been proposed for numerical modeling. In the numerical modeling, a Lagrangian approach was adopted, assuming adiabatic conditions throughout the entire PHP. The study is aligned with the investigation on analyzing the pressure and velocity variations with time for the formation and movement of plugs [3]. A U-shaped model of the pulsating heat pipe was employed to simulate oscillating heat transfer. Conservation equations were formulated for liquid and vapor slug utilizing the control volume method[6]. The internal diameter of the heat pipe of such type was constrained by the Bond Number (Bo). Since the flow inside the tube is predominantly propelled by surface tension and counteracted by gravity, the minimum value of internal diameter of the capillary is dictated by the critical diameter corresponding to be tube's Bond Number[7].

The impact of altering parameters in the adiabatic section of PHP on the start-up parameters, heat transfer performance, and diminishing dry out capability of the pulsating heat pipe was assessed by obtaining the ratio of the adiabatic region's length to the total length [8]. The experimental approach for evaluating thermal performance of the PHP was assessed with varying concentrations and fill ratios of different liquids, contrasting with deionized water. In this assessment, the calculation incorporated the effects of hydrodynamic characteristics like; viscosity and surface tension to determine an improved thermal resistance [9]. The com-

mercial software fluent was employed to account for the influence of surface tension along with phase change phenomenon on the thermal characteristics of the pulsating heat pipe. A two-phase flow model of the pulsating heat pipe was created, considering deionized water to act as the working fluid. This model, implemented on star CCM plus, did not consider temperature variations but focused on various parameters of the working fluid, operating under lower working pressure.[10] An In-house Finite volume-based Computational Fluid Dynamic (CFD) solver was used for the simulation of the oscillating motion of water at Normal Temperature Pressure (NTP) considering the filling ratio, size of tubes, and degree of temperature[11].

While numerous numerical models have been proposed over the decades, only a handful has undertaken the simulation of PHPs with water as the working fluid at normal temperature and pressure. Utilizing water performing at normal temperature and pressure, a numerical experiment was executed on Closed-loop Pulsating Heat Pipe (CLPHP). This aimed to replicate the flow dynamics, heat transfer, and temperature fluctuations arising from evaporation and condensation during the bottom heating mode[11].

The potential application of PHP technology is to be further explored at various parameters, so it is essential to compute thermal performance, as a dominating factor, of CLPHP's numerical modeling and simulation. Thus, in this research, numerical modeling is performed at NTP to simulate the flow of water volume fraction and temperature change to obtain the thermal resistance at different fill ratios of the working fluid at different heating conditions.

2. Research methodology

Research is conducted in different methods for verification and validation of the obtained data, where the experimental method is supported by a numerical method which is also shown in Figure 1.

2.1. Experimental

A PHP of the closed-loop type, featuring a single turn, was fashioned using a copper pipe with dimensions of outer diameter as 4.7625 mm and a thickness of 0.7 mm. The design of the heat pipe's diameter took into consideration the impact of surface tension and buoyancy force on the formation of slug and plug babbles. It was ensured that the diameter satisfied the critical diameter as proposed by H. Akachi[7] :

$$D \leq D_{cr} = 2 \left[\frac{\sigma}{g(\rho_f - \rho_g)} \right]^{0.5} \quad (1)$$

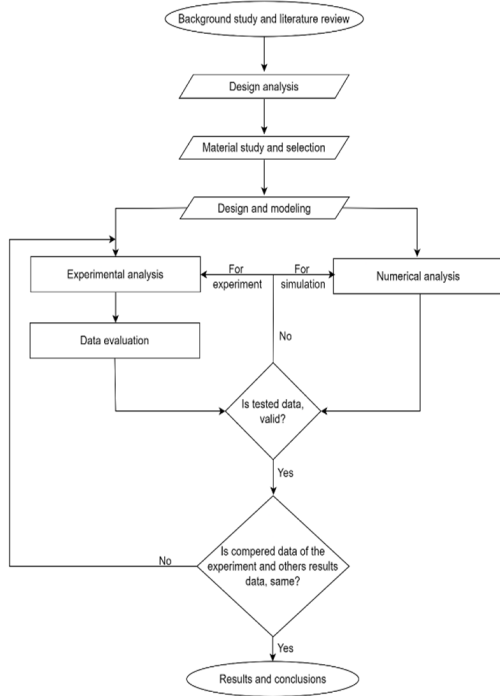


Figure 1: Research methodology flowchart.

The heat pipe is demarked into three regions: the evaporator, adiabatic, and condenser regions, each with lengths of 30mm, 140mm, and 30mm. A temperature sensor (DS18B20) is used for obtaining the data from the experiment. Temperature sensors are affixed to the walls of the condenser region, evaporator region, and the input heat source to facilitate continuous data acquisition. The experiment involves employing water as the functional fluid, and the thermal response of the pipe is observed by altering the volume of water within the copper pipe. The experiment was conducted under FRs of 40%, 50%, and 60% of the total volume. The position of the setup arrangement is shown in Figure 2.

2.2. Numerical

The numerical modeling and study are done in CFD software ANSYS Fluent where the simulation for volume fraction and the temperature difference is performed at NTP varying the FRs of working fluid (water) to examine the thermal resistance. CFD for PHP analyzes the given physical data, evaluates them, and simulates the simulation. The PHP's thermal performance was studied by varying heating conditions using commercial software for student Ansys Fluent.

Computational Fluid Dynamics (CFD) empowers researchers to simulate diverse conditions for flow and heat transfer processes that may not be easily testable. It

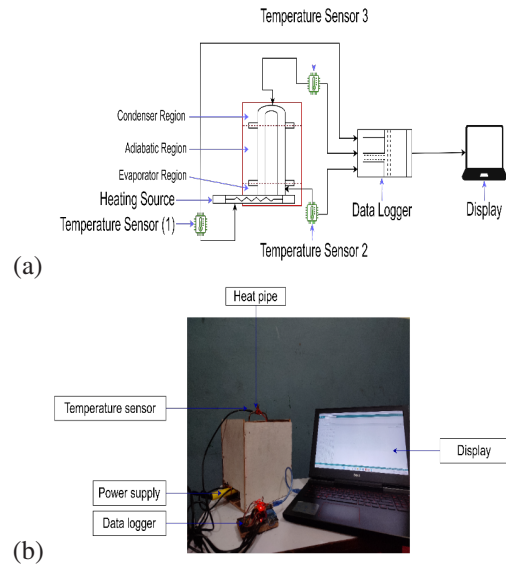


Figure 2: (a) Schematic representation of the experimental setup. (b) Experimental configuration of the setup.

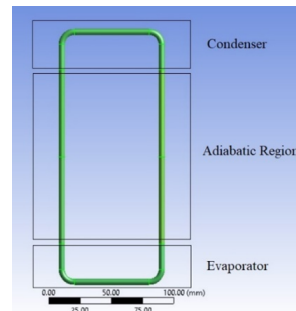


Figure 3: Geometry of single turn pulsating heat pipe

offers the capability to theoretically simulate any physical condition using computational devices[12].

2.2.1 Geometry

The geometry of this research is taken into consideration by the literature review as shown in Figure 3. A single-turn CLPHP is considered for the experiment. The critical diameter of the pipe was obtained using the equation of bond number[7]

The single-turn pulsating heat pipe is segmented into three distinct parts: the evaporator region, adiabatic region, and condenser region. The corresponding region is shown in Figure 3. The length of the condenser and evaporator are kept equal and the ratio of adiabatic to total length is obtained to be 3.5:5 [8].

2.2.2 Basic setting for the domain

The overall geometry of the PHP was primarily defined by three domains the condenser, adiabatic region, and evaporator. Water ratios of 40%, 50%, and 60% are filled in PHP and the different heating conditions are applied accordingly.

2.2.3 Boundary conditions

Various temperatures were applied to the evaporator region, specifically 393K, 398K, and 403K, In middle adiabatic region, the heat flux is maintained at zero. The numerical approach with the assisting tools of CFD utilizes the Volume of Fluid (VOF) model. In all domains, the walls are of the no-slip wall type and are assumed to be smooth. The condenser features a boundary condition involving temperature with a fixed value of 293K. Likewise, in the adiabatic regions, the boundary condition is unaltered with no heat transfer allowed, defining the heat flux as 0 W/m²K. The contact angles with walls were set to 30 degree.

2.2.4 Governing equation for VOF method

The modeling of flow inside PHP as two-phase involves slug flow in capillaries and will adhere to a general approach. This approach employs a single fluid based on VOF method. Hydrodynamics is characterized by equations governing the conservation of mass, momentum, and energy, supplemented by an additional advection equation. This advection equation is crucial for determining the gas-liquid interface in the form of the VOF[1]. The governing equation for the simulation is as follows:

Conservation of Mass:

$$\nabla \cdot \mathbf{u} = 0 \quad (2)$$

Conservation of Momentum:

$$\frac{\partial(\rho\mathbf{u})}{\partial t} + \nabla \cdot (\mathbf{u}\delta\mathbf{u}) = \nabla p + \nabla \cdot [\mu (\nabla \cdot \mathbf{u} + (\nabla\mathbf{u})^T)] + \mathbf{f}_\sigma \quad (3)$$

Conservation of Energy:

$$\frac{\delta(\rho cT)}{\delta t} + \nabla \cdot (\rho c\mathbf{u}T) = \nabla \cdot (kVT) \quad (4)$$

Here ρ denotes density, \mathbf{u} represents velocity vector, μ signifies dynamic viscosity, p stands for pressure, c represents specific heat capacity, T denotes temperature and k indicates thermal conductivity. The momentum equation's source term, \mathbf{f}_σ , represents the force due to surface tension. The governing equations are sequentially solved, and the interface is depicted utilizing the VOF method[1].

Designed for scenarios involving two or more immiscible fluids, the VOF model operated as a surface-pursuing technique on a fixed Eulerian mesh. It prioritizes tracking the precise location of the interface adjoining these fluids. Within the VOF model, a shared momentum equation set governs the fluids, and the volume fraction of all the associated fluid is continuously monitored throughout the solved domain [13].

The VOF approach of modelling is not compatible with the density-based solver, precluding the representation of void regions devoid of any fluid. In this model, one of the many phases can be identified as a compressible ideal gas, and the use of the second-order formulation which is implicit time-stepping method is not viable with the explicit VOF scheme. Modeling stream-wise continuous and circular flow, whether through a defined mass flow-rate or drop in pressure, is unattainable when employing the VOF model. Additionally, a meaningful steady-state VOF calculation is achieved solely after the solution achieves invariability of the initial conditions[14].

2.2.5 Viscous model

The k-epsilon model, a widely recognized viscous model, has been incorporated into this analysis. Like its adoption in many generic CFD programs, this model is considered a standard met for industry. Its track record includes proven stability, numerical robustness, and a well-established capacity for predictive performance. In case where generic simulations are involved, the k-epsilon model strikes a favorable balance between accuracy and precision. Within fluent, the k-epsilon viscous model employs well established two-equation models. The preference lies with the standard k-epsilon model, especially when enhanced wall treatment is applied to account for the thermal effects associated with the wall treatment [15]. The curvature correction option is selected and set as constant, and turbulence viscosity is disabled. all the values of the parameter of the viscous model are set as default as defined by Fluent.

2.2.6 Initialization

The initial conditions are set with all velocity components (u , v , and w) specified to be 0 m/s. The initial pressure is established at 101325Pa, and the initial temperature is set at 368K. This configuration is designed to accelerate the boiling of water at NTP. The operating temperature set for the simulation is 293K. The magnitude of volume fraction of water is adjusted to 1, while vapor is assigned a value of 0 and patched into their respective region.

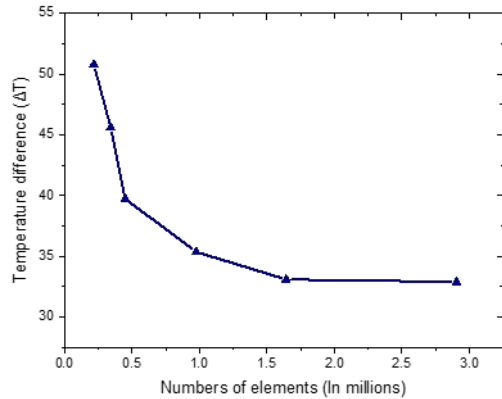


Figure 4: Grid Independent Test (GIT) of numerical modelling

2.2.7 Grid-independent test

The Grid Independence Test (GIT) involves identifying the optimal grid condition with the smallest number of grids that do not yield numerical differences in the results. This determination is made by evaluating various grid conditions.

The GIT verifies the mesh done in numerical analysis and validates it. From Figure 4, there is no significant difference in results at 0.25mm and 0.2mm. Hence element size is taken as 0.25mm at 1642578 element number as the best mesh sizing.

3. Results and conclusions

Successful completion of the research leads to appropriate results and validation and verification of the obtained data from the research. These data obtained are hence compared and discussed for their originality and proving them.

3.1. Experimental result

The experimental setup was utilized to assess the thermal performance of PHP. The thermal resistance of the particular model of PHP at the different temperatures corresponding to the FRs is figured out both through experimental and numerical methods. The phase change mechanism is verified in the pipe through the volume fraction analysis through the simulation where the change in volume of water and steam in a different region of the heat pipe is investigated. The pulsating nature of the working fluid is verified by examining the velocities of both water and vapor slugs.

3.1.1 The variation of evaporator (Te) and condenser (Tc) temperature with time

In experiments, the temperature of evaporator and also of condenser region fluctuates due to the cooling and

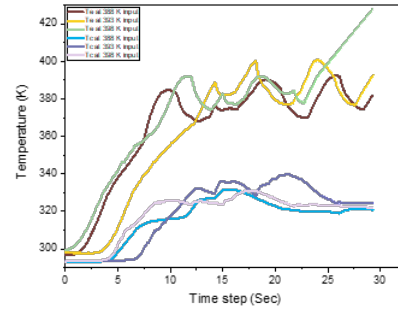


Figure 5: Variation of Te and Tc with time at 40% FR

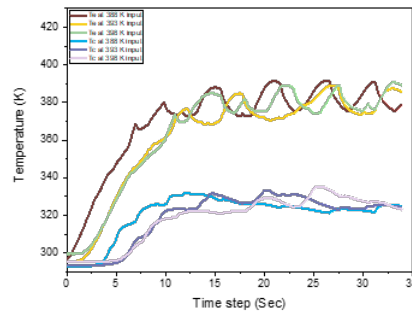


Figure 6: Variation of Te and Tc with time at 50% FR

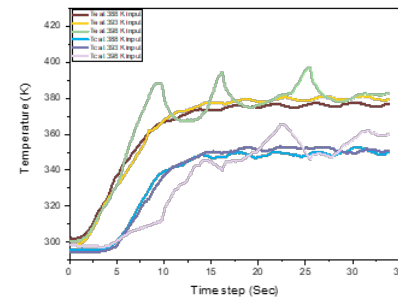


Figure 7: Variation of Te and Tc with time at 60% FR

heating of the system. Temperature changes accordingly with time, initially at the startup period the temperature at both regions isn't accurate. Following the formation of vapor and water slugs, the cooling process initiates in the evaporator, and heat is subsequently transported to another region of condenser. Consequently, the temperature gradually increases in the condenser.

The following Figure 5, Figure 6, and Figure 7 shows the temperature variation with different fill ratios (i.e., 40%, 50%, and 60% respectively). At 40% FR, notable observations reveal a sharp increase in the evaporator temperature, surpassing the 420K threshold. This pattern persists without a decline, indicating complete drying out of the fluid and a continual temperature rise.

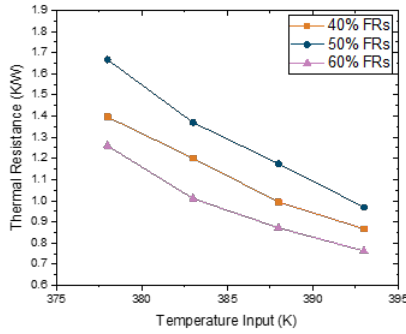


Figure 8: Variation of R_{th} with temperature inputs at different FRs at the stable case

3.1.2 Variation of R_{th} with FRs and temperature inputs

As shown in Figure 8, the simulated thermal resistance of a single-loop PHP was documented for different FRs of 40%, 50%, and 60% at temperatures of 378K, 388K, and 393K. The most striking result that emerged from the data is, the thermal resistance is the lowest at 60% FR in all three temperatures as compared to other FRs. Thermal resistance is a measurement of a material or a component's resistance to heat flow. To determine the thermal resistance of PHP, the thermal energy supplied are divided by the temperature difference between the two separate sections, evaporator and condenser. The PHP's thermal resistance is established by dividing the temperature differential between these regions by the associated heating power.[6]

$$R = \frac{T_e - T_c}{Q} \quad (5)$$

Here, T_e denotes the mean temperature of the evaporator whereas T_c represents the mean temperature of the condenser.

The experiment is conducted to figure out the R_{th} of the heat pipe varying the FRs and temperature inputs. The initiation mechanism holds significant importance in the thermal performance of the PHP, which governs the oscillating flow inside the fluid domain of PHP[4]. While in startup state, unstable data is obtained and after a few times, the system is stable hence the experimented data. After a few times steps following the initial oscillation, accurate data is obtained, and Figure 8 below illustrates the thermal resistance under stable conditions. The impact of surface tension, specific heat capacities, latent heat of vaporization, and viscosity on the thermal performance of the PHP fluctuates with varying fill ratios and heating load conditions[16].

Surface tension significantly amplifies capillary resistance and influences the contact angle between the working fluid and the tube wall. This elevation in capillary

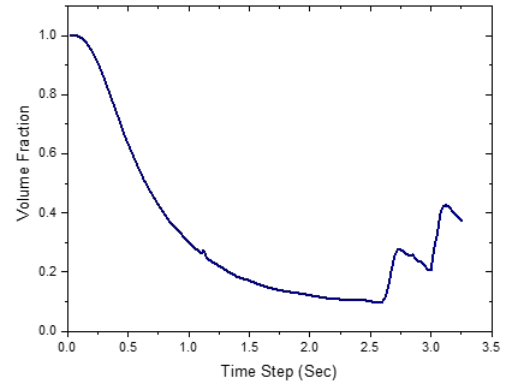


Figure 9: Deviation of water volume fraction within evaporator at time step (s)

resistance ultimately diminishes heat transfer[2].

3.2. Numerical result

Numerical analysis is performed in Ansys Fluent for different heating conditions. Different parameters such as phase change, water volume flow behavior, and pulsating nature of heat pipe validate the obtained data with the experimentally obtained data. Various Contours are observed and calculated to obtain different parameters of the experiment through the simulation. Data are recorded as per time step since the simulations are performed at a transient state.

3.2.1 Phase change

The determination of phase change in various regions of the heat pipe relies on the alteration of volume fraction of two phases of functional fluid. An observable shift in volume of water or steam serves as evidence of a phase change occurring inside the tube.

The oscillating flow inside the PHP fluctuates the temperature in different regions. The anticipated outcome unfolds as follows: the temperature in the evaporator decreases as heat is transferred to the condenser through the oscillation of water vapor. Concurrently, the temperature in the condenser rises. The observed temperature fluctuation in both the evaporator and condenser regions validate the existence of a heat exchange mechanism with the tube.

The above Figure 9 significantly describes the change of phase of the PHP. Initially, the water volume fraction is 1 in the evaporator region and gradually decreases due to the phase change of water into the steam. After 2.625s, condensation of steam leads to an augmentation in the water volume fraction, allowing for the observation of the phase change in the PHP.

The thermal resistance experiences a rapid decrease, followed by a significant slowing of the rate. Once the

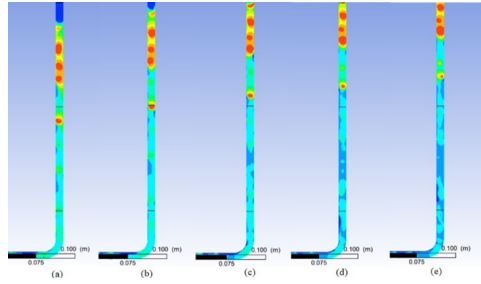


Figure 10: Formation of water and vapor slug formation at PHP at (a) 1.1 sec (b) 1.2 sec (c) 1.3 sec (d) 1.4 sec (e) 1.5 sec

phase change is initiated, attained at distinct heat supply levels for different fluids, contingent upon operational pressure and boiling point, the PHP endures a remarkable reduction in thermal resistance. This phenomenon is attributed to the abundant availability of heat, facilitating the onset of intense boiling, and consequently leading to a notable decline in the thermal resistance of PHP[17].

3.2.2 Water volume flow behavior

The pulsating flow inside PHP was obtained from the simulation using ANSYS 2022 R2 Fluent’s volume of the multiphase model to study its thermal performance at various heating conditions. The oscillating motion of liquid and vapor plugs is effectively replicated through numerical modeling.

Figure 10 illustrates the oscillation of the volume fraction of vapor within the PHP. At a heat pipe with liquid and vapor plug at PHP filled with 50% water, the vapor slug rises from the evaporator and transitions to vapor-liquid plug flow as illustrated in Figure 10 (a). The performance of a PHP is significantly subjective by the surface tension of the fluid that aids in the formation of self-sustained liquid and vapor plugs. The oscillation characteristics during the initiation of loop operation facilitate heat transport, allowing pulsation from the heating to the cooling section[2].

3.2.3 Velocity

For a heat pipe to be pulsating in nature, the velocity of the fluid must be in both directions in the y-axis in certain time steps at the same section of the tube. The flow visualization through the simulation considers the velocity vector of the working fluid.

The cross-section of the pipe which is the same for all the data of the velocity vector is shown in Figure 11. Within the heat pipe, a designated plane is defined, and it is on this plane that the observation of fluid velocity occurs, corresponding to the cross-sectional area. Figure 12 depicts the fluid velocity in two opposing

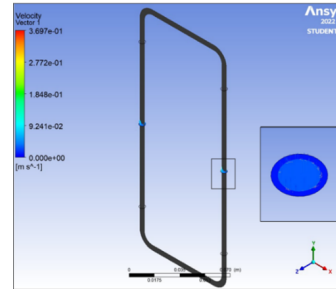


Figure 11: Cross-sectional plane of heat pipe contour.

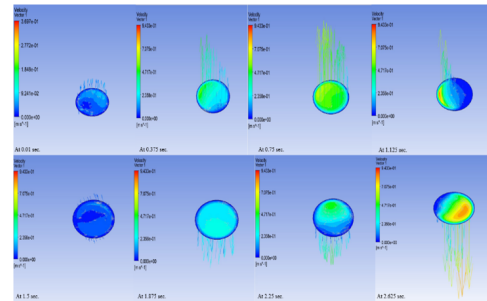


Figure 12: Fluid velocity at different time steps in the same cross-sectional plane of the heat pipe.

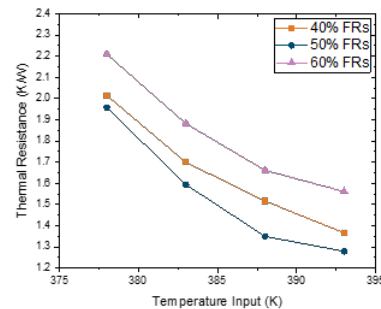


Figure 13: Variation of R_{th} with temperature inputs at different FRs (Numerical analysis)

directions at different time intervals within the same direction of the pipe. This observation confirms the pulsating nature of the heat pipe.

3.3. Validation of obtained result

The thermal performance of the modeled PHP is obtained by simulating the experiment using Ansys Fluent. The experiment was simulated for different FRs and temperature inputs. Since the simulation was of a small period, which shows the startup phase. The R_{th} obtained from the experiment and the simulated data are compared for the startup period for both cases. From Figure 13 and Figure 14, it can be interpreted that R_{th} at 393K at a 50% FR is the best for both experimental and numerical modeling followed by 40% and 60% respec-

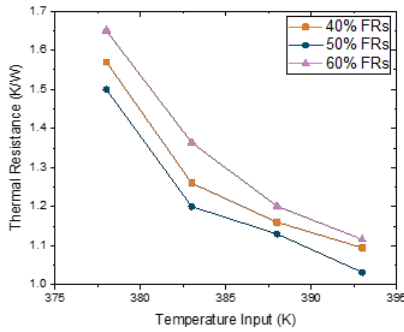


Figure 14: Variation of R_{th} with temperature inputs at different FRs (Experimental analysis)

Table 1: Comparison of experimental and reference data and their errors

FRs	Experimental data (R_{th})	D. Baitule and P. Pachghare's experimental data (R_{th})	Error
50%	0.969	1.15	15.73%
60%	0.762	0.82	7.07%

tively. In both models, thermal resistance is the lowest at 393K. The obtained results align with previous research; in comparison to another article, they indicate that the thermal resistance declines with a surge in temperature inputs. The most striking result that emerged from the data is, that at a 50% fill ratio, the thermal resistance is at its minimum[18].

For verification of the data, the experimental data obtained are compared with the recent experiments performed by other researchers. Comparisons are made for the thermal resistance of the PHP at FRs of 40%, 50%, and 60%. The thermal resistance for a 60% FR, obtained from the experimental data of D. Baitule and P. Pachghare, is approximately 45W at 393K input for water, which aligns closely with the experimentally obtained data presented in Table 1. Table 1 presents us with the data comparison of the experiment with D. Baitule and P. Pachghare's data[19]. The lowest thermal resistance achieved is equivalent to each other. Hence through this validation, the error is found to be 7.073% at the lowest thermal resistance. The deviation of the data and the error may occur due to differences in surface area, ambient temperature, loss of input heat, and the steady state time for the experiment.

The evaporator and condenser's temperature varies with heat applied along with the working fluid. The data obtained from the experiment is presented in Figure 15

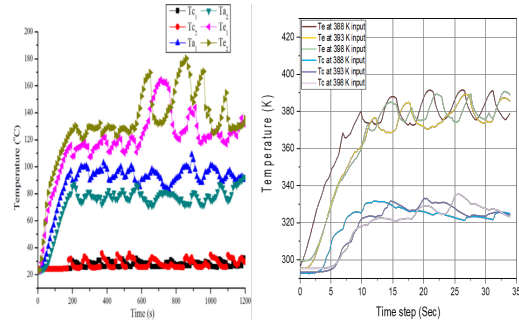


Figure 15: Comparison of the temperature fluctuation; J. Wang's experiment at 50% FR, at 40W with regular PHP with the experimentally obtained data at similar case [20].

which is compared with the data graph of J. Wang at 50% fill ratio[20]. Table 1 presents us with the data comparison of the experiment with D. Baitule and P. Pachghare's data[19]. The lowest thermal resistance achieved is equivalent to each other. Hence through this validation, the error is found to be 7.073% at the lowest thermal resistance. The deviation of the data and the error may occur due to differences in surface area, ambient temperature, loss of input heat, and the steady state time for the experiment. The evaporator and condenser's temperature varies with heat applied along with the working fluid. The data obtained from the experiment is presented in Figure 15 which is compared with the data graph of J. Wang at 50% fill ratio[20].

4. Conclusion

The experiment has given an account of experimental modeling and numerical modeling in single-turn PHP under different heating conditions in ANSYS fluent. It was conducted with 40%, 50%, and 60% FRs at 388K, 393K, and 398K temperatures. The PHP's thermal resistance was derived across all the mentioned cases. Thermal resistance obtained from the simulation and the experiment are relatively the same for the startup case. Further data collection through simulation is required to visualize the continuous flow of water and vapor plug since the simulation was only possible for 3.25s. The velocity of the fluid was observed at a cross-section of a pipe for different time steps. The following conclusion has been made from the experiment:

1. Comprehensive results of PHP's thermal resistance by varying FRs at different heating conditions experimentally which is the best for a 60% FR at 393K were obtained.
2. The evidence of the heat-transferring mechanism of PHP through the study of temperature obtained

from the experimental and numerical modeling was provided by the experiment.

3. The water flow behavior and formation of vapor and liquid slugs were confirmed through the numerical modeling of the volume fraction contour for water phase.
4. The phase change of fluid was proved by changing the liquid phase volume fraction in the evaporator at varying time intervals.

The findings of this study suggest that the fluid in the PHP undergoes oscillating flow from the velocity vector contour of the fluid and also from numerical modeling and this is effective for cooling systems. The implications of other operation parameters can be studied further to fully understand the chaotic flow nature of PHP.

Acknowledgement

We extend our heartfelt gratitude to the Department of Mechanical and Automobile Engineering for their invaluable support in facilitating the experiment and providing technical assistance.

References

- [1] Venkata Suresh J, Bhramara P. Cfd analysis of multi-turn pulsating heat pipe[C/OL]// Materials Today: Proceedings. Elsevier Ltd, 2017: 2701-2710. DOI: [10.1016/j.matpr.2017.02.146](https://doi.org/10.1016/j.matpr.2017.02.146).
- [2] Khandekar S, Panigrahi P K, Lefèvre F, et al. Local hydrodynamics of flow in a pulsating heat pipe: A review[J/OL]. Frontiers in Heat Pipes, 2010, 1(2). DOI: [10.5098/fhp.v1.2.3003](https://doi.org/10.5098/fhp.v1.2.3003).
- [3] Han X, Wang X, Zheng H, et al. Review of the development of pulsating heat pipe for heat dissipation[J/OL]. Renewable and Sustainable Energy Reviews, 2016, 59: 692-709. DOI: [10.1016/j.rser.2015.12.350](https://doi.org/10.1016/j.rser.2015.12.350).
- [4] Bastakoti D, Zhang H, Li D, et al. An overview on the developing trend of pulsating heat pipe and its performance[J/OL]. Applied Thermal Engineering, 2018, 141: 305-332. DOI: [10.1016/j.rser.2015.12.350](https://doi.org/10.1016/j.rser.2015.12.350).
- [5] Pouryoussefi S M, Zhang Y. Numerical investigation of chaotic flow in a 2d closed-loop pulsating heat pipe[J/OL]. Appl Therm Eng, 2016, 98: 617-627. DOI: [10.1016/j.applthermaleng.2015.12.097](https://doi.org/10.1016/j.applthermaleng.2015.12.097).
- [6] Mohammadi M, Ghahremani A R, Shafii M B, et al. Experimental investigation of thermal resistance of a ferrofluidic closed-loop pulsating heat pipe[J/OL]. Heat Transfer Engineering, 2014, 35(1): 25-33. DOI: [10.1080/01457632.2013.810086](https://doi.org/10.1080/01457632.2013.810086).
- [7] Akachi H. Structure of a heat pipe: 4921041[P]. 1990.
- [8] Li Q, Wang C, Wang Y, et al. Study on the effect of the adiabatic section parameters on the performance of pulsating heat pipes[J/OL]. Appl Therm Eng, 2020, 180. DOI: [10.1016/j.applthermaleng.2020.115813](https://doi.org/10.1016/j.applthermaleng.2020.115813).
- [9] Bastakoti D, Zhang H, Cai W, et al. An experimental investigation of thermal performance of pulsating heat pipe with alcohols and surfactant solutions[J/OL]. Int J Heat Mass Transf, 2018, 117: 1032-1040. DOI: [10.1016/j.ijheatmasstransfer.2017.10.075](https://doi.org/10.1016/j.ijheatmasstransfer.2017.10.075).
- [10] Nagwase S Y, Pachghare P R. 2013 international conference on energy efficient technologies for sustainability (iceets)[C/OL]// IEEE. 2013. DOI: [10.1109/ICEETS.2013.6533380](https://doi.org/10.1109/ICEETS.2013.6533380).
- [11] Sharma M, Sikarwar B S. Flow and heat transfer of fluid in a pulsating heat pipe[J/OL]. Journal of Physics: Conference Series, 2019. DOI: [10.1088/1742-6596/1369/1/012019](https://doi.org/10.1088/1742-6596/1369/1/012019).
- [12] Bitencourt U C, Khounsary P A. Cfd simulation of a pulsating heat pipe using ansys fluent a paper submitted as a part of a research project entitled 'development of a pulsating heat pipe for enhanced heat transfer'[R]. 2016.
- [13] Eghbalzadeh A, Javan M. Comparison of mixture and vof models for numerical simulation of air-entrainment in skimming flow over stepped spillways[J/OL]. Procedia Engineering, 2012: 657-660. DOI: [10.1016/j.proeng.2012.01.786](https://doi.org/10.1016/j.proeng.2012.01.786).
- [14] Ansys[EB/OL]. 1971. <https://www.ansys.com/products/3d-design>.
- [15] Al-Witry A, Es-Saheb M. Benchmarking the performance of the ansys-fluent standard k- turbulence model in fluid flow and heat transfer predictions for complex flows around circular pin-fins using various near wall functions[J/OL]. Research Journal of Applied Sciences, Engineering and Technology, 2013, 5(17): 4301-4310. DOI: [10.19026/rjaset.5.4421](https://doi.org/10.19026/rjaset.5.4421).
- [16] Wasankara V K, Pachghare P R. Effect of surface tension on the thermal performance of pulsating heat pipe: A review[J/OL]. 2020. DOI: [10.1051/e3sconf/202339101031](https://doi.org/10.1051/e3sconf/202339101031).
- [17] Yang Y M, Maa J R. Pool boiling of dilute surfactant solutions[J/OL]. 1983. DOI: doi.org/10.1115/1.3245541.
- [18] Guragain K, Badu P, Bastakoti D. Computational analysis of single-loop heat pipe for predicting thermal resistance. thermal performance of pulsating heat pipe[J/OL]. Conference on Recent Trends Of Science, Technology, And Innovation (RTSTI) 2023 Prithvi Narayan Campus, Pokhara, 2023. DOI: [10.13140/RG.2.2.30818.50885](https://doi.org/10.13140/RG.2.2.30818.50885).
- [19] Baitule D A, Pachghare P R. Experimental analysis of closed loop pulsating heat pipe with variable filling ratio[J/OL]. 2013. DOI: [10.1016/j.egypro.2015.07.665](https://doi.org/10.1016/j.egypro.2015.07.665).
- [20] Wang J, Ma H, Zhu Q, et al. Numerical and experimental investigation of pulsating heat pipes with corrugated configuration[J/OL]. Appl Therm Eng, 2016, 102: 158-166. DOI: [10.1016/j.applthermaleng.2016.03.163](https://doi.org/10.1016/j.applthermaleng.2016.03.163).